

The r -Process in the Proto-Neutron-Star Winds with Anisotropic Neutrino Emission

Shinya Wanajo

*Department of Astronomy, School of Science, University of Tokyo, Bunkyo-ku, Tokyo, 113-8654, Japan;
wanajo@astron.s.u-tokyo.ac.jp*

ABSTRACT

The astrophysical origin of the r -process nuclei is still unknown. Even the most promising scenario, the neutrino-driven winds from a nascent neutron star, encounters severe difficulties in obtaining requisite entropy and short dynamic timescale for the r -process. In this study, the effect of anisotropy in neutrino emission from a proto-neutron star surface is examined with semi-analytic neutrino-driven wind models. The increase of neutrino number density in the wind owing to the anisotropy is modeled schematically by enhancing the *effective* neutrino luminosity. It is shown that the neutrino heating rate from neutrino-antineutrino pair annihilation into electron-positron pairs can significantly increase owing to the anisotropy and play a dominant role for the heating of wind material. A factor of five increase in the effective neutrino luminosity results in 50% higher entropy and a factor of ten shorter dynamic timescale owing to this enhanced neutrino heating. The nucleosynthesis calculations show that this change is enough for the robust r -process, producing the third abundance peak ($A = 195$) and beyond. Future multi-dimensional studies with accurate neutrino transport will be needed if such anisotropy relevant for the current scenario (more than a factor of a few) is realized during the wind phase ($\sim 1 - 10$ s).

Subject headings: nuclear reactions, nucleosynthesis, abundances — stars: abundances — stars: neutron — supernovae: general

1. Introduction

The astrophysical site of the rapid-neutron-capture nucleosynthesis (r -process), which accounts for about half of nuclei heavier than iron, has been a long-standing mystery. During the last decade, the neutrino-heated ejecta from a nascent neutron star (neutrino-driven winds, Woosley et al. 1994) has been considered to be the most promising astrophysical site for the r -process. Previous studies show, however, severe problems in obtaining requisite high entropy and short dynamic timescale for the production of heavy r -process nuclei (Qian & Woosley 1996; Otsuki et al. 2000; Sumiyoshi et al. 2000; Wanajo et al. 2001; Thompson et al. 2001). The general relativistic effect for a very compact proto-neutron star (e.g., the mass of $2.0 M_{\odot}$ with the radius of 10 km, Otsuki et al. 2000; Wanajo et al. 2001) or a magnetar-like magnetic field strength (Thomp-

son 2003; Suzuki & Nagataki 2005) have been invoked to increase entropy and reduce the dynamic timescale of the winds. It is questionable, however, if such physical conditions can be the general requirements for the r -process nucleosynthesis.

Qian & Woosley (1996) have suggested that an additional energy input to the neutrino-driven wind at between 1.5 and 3 times the neutron star radius is efficient to increase entropy and reduce dynamic timescale of the wind material. In this *Letter*, it is shown that strong anisotropy in neutrino emission from the proto-neutron star, *if it exists*, acts as this extra energy source and helps the r -process. The neutrino-driven wind model with spherically symmetric, steady outflow approximation is used to obtain the wind trajectories (§ 2). A sudden increase of neutrino number density in winds owing to anisotropic neutrino emission is modeled by enhancing the neutrino lumi-

osity. Nucleosynthesis calculations with the obtained thermodynamic trajectories are performed to demonstrate this effect (§ 3). Finally, a possible origin of this anisotropy in neutrino emission and some implications of this study are discussed (§ 4).

2. Wind Models with Anisotropic Neutrino Emission

The wind trajectories in this study are obtained using the semi-analytic, general relativistic model of neutrino-driven winds explored in Otsuki et al. (2000) and Wanajo et al. (2001, 2002). In this model, the system is treated as time stationary and spherically symmetric, and the radius of the neutron star is assumed to be the same as that of the neutrino sphere. The heating source that drives matter from the neutrino sphere is due to neutrino interactions. Heating is due to ν_e and $\bar{\nu}_e$ capture on free nucleons ($\dot{q}_{\nu N}$), neutrino scattering by electrons and positrons ($\dot{q}_{\nu e}$), and neutrino-antineutrino pair annihilation into electron-positron pairs ($\dot{q}_{\nu\nu}$). Cooling is due to electron and positron capture on free nucleons (\dot{q}_{eN}) and electron-positron pair annihilation into neutrino-antineutrino pairs (\dot{q}_{ee}). The rms average neutrino energies are taken to be 10, 20, and 30 MeV, for electron, anti-electron, and the other flavors of neutrinos, respectively. The mass ejection rate at the neutrino sphere \dot{M} is determined so that the wind becomes supersonic through the sonic point.

The mass and radius of the neutron star are taken to be $M = 1.4 M_\odot$ and $R = 10$ km, respectively. The neutrino luminosity of one specific flavor is assumed to be the same for all other flavors, which is taken to be a constant value $L_\nu = 1 \times 10^{51} \text{ erg s}^{-1}$. Note that the assumption of a constant L_ν is reasonable, since the crossing time of a wind over the heating region (< 30 km, see Fig. 2) is short enough, ~ 0.1 s, compared to the decay timescale of L_ν (a few seconds, e.g., Woosley et al. 1994). As explored in previous studies, this *typical* choice of parameter set (with isotropic neutrino emission) results in insufficient physical conditions (i.e., low entropy and long dynamic timescale) for the production of heavy r -process nuclei (e.g., Wanajo et al. 2001).

In this study, anisotropy in neutrino emission

is modeled schematically as follows. Given there is substantially higher neutrino emission from the “hot spot”, which is marked by the point P_1 ($OP_1 = R$) in Figure 1. At the point P_0 ($OP_0 = R$) nearby P_1 , the ejection of matter is due to the local (lower) isotropic neutrino emission around P_0 . The matter suddenly sees a substantially larger number of neutrinos when passing through the point P_2 . Note that neutrino emission at an arbitrary point on the neutrino sphere (e.g., P_0 or P_1) is assumed to be isotropic in all directions (i.e., the local neutrino flux is *not* radial) as in Otsuki et al. (2000). This sudden increase of the neutrino number density at P_2 is approximated by a jump of the neutrino luminosity from the original value $L_\nu = 1 \times 10^{51} \text{ erg s}^{-1}$ for $R < r < R_2$ to the *effective* luminosity $L_{\nu 2}$ for $r \geq R_2$, where r is the distance from the center O and $R_2 = OP_2$.

The wind models considered in this study are listed in the first column of Table 1, where R_2 (second column) and $L_{\nu 2}$ (third column) are taken to be 10, 12, 15, and 20 km, and 1.0, 2.0, 3.0, 4.0, and 5.0 in units of $10^{51} \text{ erg s}^{-1}$. The resulting net heating rate (\dot{q} ; *top panel*) for models A1, A5, B5, C5, and D5 and each heating/cooling rate (*bottom panel*) for models A5 and B5 are shown in Figure 2, as functions of r . Note that A1-A5 are *isotropic* wind models (i.e., $R_2 = R$).

For isotropic winds (A1-A5 in Table 1), the higher $L_{\nu 2}$ ($= L_\nu$ in these cases) results in shorter dynamic timescale τ_{dyn} ($\equiv |\rho/(d\rho/dt)|_{T=0.5 \text{ MeV}}$) and *lower* asymptotic (i.e., maximum) entropy s . This shows that the increased \dot{q} (see A1 and A5 in Fig. 2, *top panel*) is consumed to drive more matter (i.e., higher \dot{M} as can be seen in Table 1) from the neutron star surface with faster velocity, rather than to increase entropy. In contrast, for anisotropic models, an increase of $L_{\nu 2}$ (for $r \geq R_2$) is quite efficient *both* to increase entropy and to reduce dynamic timescale (Table 1). The reason is that the matter has been already lifted with low L_ν ($= 1 \times 10^{51} \text{ erg s}^{-1} < L_{\nu 2}$) and thus with small \dot{M} . Therefore, the density (and temperature) at arbitrary r is significantly small compared to the corresponding isotropic wind. This can be seen in the 5th (and 6th) column in Table 1, which lists the density ρ_{13} (and temperature T_{13}) at $r = 13$ km (see about one order difference in ρ_{13} for A5 and B5).

For isotropic wind models, the five times greater

neutrino luminosity simply results in the increase of \dot{q} with the same factor (A1 and A5 in Fig. 2, *top panel*). This does not hold, however, for anisotropic wind models. For model B5, the maximum \dot{q} is as twice large as that for model A5 (with the same $L_{\nu 2}$), and more than 10 times larger than that for model A1 (with the same L_{ν}). This can be explained as follows. As shown in Figure 2 (*bottom panel*), for isotropic winds (*dashed lines*; A5), the heating is mainly due to $\dot{q}_{\nu N}$ and $\dot{q}_{\nu e}$, while $\dot{q}_{\nu\nu}$ plays only a minor role. In contrast, for anisotropic winds (*solid lines*; B5), the neutrino pair annihilation $\dot{q}_{\nu\nu}$ plays a crucial role, whose peak (at $r \approx 13$ km) is a factor of seven higher than that in A5. This effect can be clearly seen in Figure 2 (*top panel*), in which the case without an increase of $\dot{q}_{\nu\nu}$ (model B5a) and with an increase of $\dot{q}_{\nu\nu}$ only (model B5b) are compared (see also Table 1).

This is due to the difference of ρ and T dependences in these heating terms. For a fixed set of r , Y_e , L_{ν} and neutrino mean energies, these heating rates are related to ρ and T such as $\dot{q}_{\nu N} = \text{constant}$, $\dot{q}_{\nu e} \propto T^4 \rho^{-1}$, and $\dot{q}_{\nu\nu} \propto \rho^{-1}$ (Qian & Woosley 1996; Otsuki et al. 2000). As a result, $\dot{q}_{\nu N}$ in B5 (Fig. 2, *bottom panel*) closely follows that in A5 for $r > R_2$, which is independent of ρ and T . As can be seen in Table 1, a reduction in ρ owing to low L_{ν} in B5 (compared to that in A5) is accompanied with a reduction in T . As a consequence, $\dot{q}_{\nu e}$ in B5 is lower than that in A5 even for $r > R_2$. However, $\dot{q}_{\nu\nu}$ is not dependent on T but is inversely proportional to ρ (i.e., proportional to the number of neutrinos per volume), which becomes significantly high owing to the decreasing ρ for $r > R_2$ (Table 1). Note that the cooling terms ($\dot{q}_{eN} \propto T^6$ and $\dot{q}_{ee} \propto T^9 \rho^{-1}$) quickly decay with increasing r and have negligible effects by the anisotropy (Fig. 2).

As can be seen in the above numerical experiments, the strong anisotropy in neutrino emission can be an additional energy source pointed out by Qian & Woosley (1996). However, this mechanism may work only for $r < 1.5 R$, which is rather closer to the neutrino sphere than the suggested range ($1.5 < r/R < 3$) by Qian & Woosley (1996). In the current study, the effects of increasing entropy and accelerating wind are prominent for the wind closer to the hot spot, in particular for $R \approx 12$ km (Table 1), at which \dot{q} maxi-

mizes (Fig. 2). The effect of anisotropic neutrino emission becomes less important for a more distant wind (e.g., $R_2 = 20$ km), where the neutrino heating has mostly ceased (Fig. 2). For a fixed R_2 , the effect is more significant for higher $L_{\nu 2}$ as can be seen in Table 1. For model B5, the entropy is about 50% higher ($180 N_A k$) and the dynamic timescale is about a factor of ten shorter (1.65 ms) than those in the isotropic model A1 with the same L_{ν} ($s = 117 N_A k$ and $\tau_{\text{dyn}} = 14.1$ ms).

Note that the purely parametric examinations explored in this section should be regarded as only qualitative ones. For instance, the “hot spot” is not necessary a point as illustrated in Figure 1. It is conceivable that the area with strong neutrino emission has some distribution on the neutrino sphere. Moreover, the configuration should become multi-dimensional soon after the wind material passes the point P₂ in Figure 1, which is treated within the framework of a spherical wind model in the current study. More realistically, the wind matter deviates from the radial to the direction of OP₂ in Figure 1. This may moderate the acceleration of wind and increase the heating duration. Hence, the current results may overestimate the reduction of dynamic timescale and underestimate the increase of entropy. It is difficult to estimate the net effect to the nucleosynthesis from these modifications. Obviously, a multi-dimensional approach will be needed to quantitatively estimate the effects of the anisotropy.

3. Nucleosynthesis in Winds

Adopting the wind trajectories discussed in § 2 for the physical conditions, the nucleosynthetic yields are obtained by solving an extensive nuclear reaction network. The network consists of 6300 species between the proton and neutron drip lines (for more detail, see Wanajo 2006). Neutrino-induced reactions and nuclear fission are not considered in the current study. Each calculation is initiated when the temperature decreases to $T_9 = 9$ (where $T_9 \equiv T/10^9$ K). The initial compositions are given by $X_n = 1 - Y_e$ and $X_p = Y_e$, respectively, where X_n and X_p are the mass fractions of neutrons and protons, and Y_e is the initial electron fraction (number of proton per nucleon) at $T_9 = 9$. In this study, Y_e is taken to be 0.4, according to the core-collapse simulation in Woosley

et al. (1994, at $L_\nu \approx 1 \times 10^{51} \text{ erg s}^{-1}$). As in Wanajo et al. (2002), the temperature and density are set to be constant when T_9 decreases to 1.0, in order to mimic the effect of the slower outgoing ejecta behind the shock.

The nucleosynthesis results for models B2-B5, C2-C5, and D2-D5 (Table 1) are shown in Figure 3, as a function of atomic mass number. For anisotropic wind models with $R_2 = 12 \text{ km}$ (B2-B5), the effect of anisotropic neutrino emission is evident. A factor of three or four increase in $L_{\nu 2}$ (B3 and B4 in Table 1) leads to $s \approx 150 - 160 N_A k$ and $\tau_{\text{dyn}} \approx 3 - 4 \text{ ms}$, resulting in the r -process nucleosynthesis (Fig. 3). For model B5, the high entropy ($= 180 N_A k$) and short dynamic timescale ($= 1.65 \text{ ms}$) of the wind drive the nuclear matter to the actinide region. The neutron-to-seed abundance ratio at the beginning of the r -process, defined as $T_9 = 2.5$, is $Y_n/Y_h = 176$ and the final averaged mass number of heavy nuclei with $Z > 2$ is $\langle A_h \rangle = 230$ (Table 1). For the models with $R_2 = 15 \text{ km}$ (C2-C5), the r -process still takes place when $L_{\nu 2}$ is four or five times higher than L_ν (models C4 and C5). For $R_2 = 20 \text{ km}$ (D2-D5), the effect of anisotropic neutrino emission is not important and the nucleosynthesis results are not significantly different from the isotropic cases (A1-A5).

4. Implications

In this *Letter*, the effects of anisotropy in neutrino emission for the r -process nucleosynthesis in proto-neutron-star winds were examined, using the spherically symmetric, steady outflow model of neutrino-driven winds. It was shown that strong anisotropy, *if it exists*, can be an additional energy source (Qian & Woosley 1996) to heat the wind material. A factor of four or five enhancement in *effective* neutrino luminosity results in the significant increase of entropy and shortening of dynamic timescale of outgoing neutrino-heated ejecta. This is mainly due to the *boosted* neutrino heating from annihilation of neutrino-antineutrino pairs into electron-positron pairs as a result of anisotropic neutrino emission. This provides the physical condition suitable for the robust r -process, producing the third abundance peak ($A = 195$) and beyond.

It is conceivable that asymmetric neutrino

emission can be associated with the anisotropic matter distribution near the neutrino sphere. As an example, Kotake et al. (2003) suggested that the non-spherical neutrino sphere owing to rapid rotation leads to anisotropic neutrino heating with the pole-to-equator ratio of a few to more than 10. This may result in strong contrast in neutrino emission on the neutrino sphere, which forms an *effective* “hot spot” around the rotational axis. A recent work with more sophisticated neutrino-transport scheme by Walder et al. (2005) showed, however, that the pole-to-equator flux ratio is at most a factor of two, even for a rather rapidly rotating core. This is a consequence that the radiation field is smoothened by the many neutrino sources above the neutrino sphere (e.g., convective bubbles) at the early phase ($< 1 \text{ s}$ after core bounce). Nevertheless, all the convective bubbles are evacuated during the late wind phase ($\sim 10 \text{ s}$) and a strong contrast of neutrino flux might form on the neutrino sphere for a rapidly rotating core.

Another possibility of anisotropic neutrino emission might be due a global fluid instabilities of neutrino-heated matter as observed in multi-dimensional hydrodynamic simulations. Recent works have shown that hydrodynamic instabilities can lead to low-mode ($l = 1$ in terms of an expansion in spherical harmonics of order l) oscillation of the convective fluid flow in the neutrino-heated layer behind the shock (e.g., Scheck et al. 2006; Buras et al. 2006b; Burrows et al. 2006). The presence of such a low convective mode results in the pair of a single outflow and a narrow accretion flow that creates the “hot spot” on the neutron star surface. It should be noted, however, that the two-dimensional simulations by Scheck et al. (2006) showed that the anisotropy of the accretion luminosity owing to this flow appears to be only a few percent (at least during the early phase up to $\sim 1 \text{ s}$ after core bounce). A future investigation relevant for the wind phase ($\sim 1 - 10 \text{ s}$) will be needed to examine the degree of anisotropic neutrino emission from such an accretion flow.

Given one of the above (or another unknown) mechanism works, a constraint for the r -process may be obtained from the condition that creates the “hot spot” owing to, e.g., rapid rotation or long lasting accretion flow. It is conceivable that only a limited fraction of supernovae create the “hot spot” relevant for the current scenario (e.g.,

rapid rotators or less-energetic supernovae that form the long lasting accretion flow). This can be a reasonable explanation for that the spectroscopic analysis of extremely metal-poor stars and Galactic chemical evolution study imply only a limited fraction of core-collapse supernovae undergo the r -process nucleosynthesis (Ishimaru & Wanajo 1999; Ishimaru et al. 2004).

The implications in this study must be tested by future multi-dimensional simulations of core-collapse supernovae for long duration (~ 10 s) with accurate neutrino transport. Systematic calculations of nucleosynthesis with such hydrodynamic trajectories will be also needed to investigate the contribution to the Galactic chemical evolution of r -process nuclei.

I would like to acknowledge H. -Th. Janka for helpful discussions. I also acknowledge the contributions of an anonymous referee, which led to clarification of a number of points in the original manuscript. This work was supported in part by a Grant-in-Aid for Scientific Research (17740108) from the Ministry of Education, Culture, Sports, Science, and Technology of Japan.

REFERENCES

- Buras, R., Rampp, M., Janka, H. -Th., & Kifonidis, K. 2006a, *A&A*, 447, 1049
- Buras, R., Janka, H. -Th., Rampp, M., Kifonidis, K. 2006b, *A&A*, submitted (astro-ph/0512189)
- Burrows, A., Livne, E., Dessart, L., Ott, C. D., & Murphy, J. 2006, *ApJ*, 640, 878
- Ishimaru, Y. & Wanajo, S. 1999, *ApJ*, 511, L33
- Ishimaru, Y., Wanajo, S., Aoki, W., & Ryan, S. G. 2004, *ApJ*, 600, L47
- Kotake, K., Yamada, S., & Sato, K. 2003, *ApJ*, 595, 304
- Otsuki, K., Tagoshi, H., Kajino, T., & Wanajo, S. 2000, *ApJ*, 533, 424
- Qian, Y. -Z. & Woosley, S. E. 1996, *ApJ*, 471, 331
- Scheck, L., Kifonidis, K., Janka, H. -Th., Müeller, E. 2006, *A&A*, submitted (astro-ph/0601302)
- Sumiyoshi, K., Suzuki, H., Otsuki, K., Terasawa, M., & Yamada, S. 2000, *PASJ*, 52, 601
- Suzuki, T. K. & Nagataki, S. 2005, *ApJ*, 628, 914
- Thompson, T. A., Burrows, A., & Meyer, B. S. 2001, *ApJ*, 562, 887
- Thompson, T. A. 2003, *ApJ*, 585, L33
- Walder, R., Burrows, A., Ott, C. D., Livne, E., Lichtenstadt, I., & Jarrah, M. 2005, *ApJ*, 626, 317
- Wanajo, S., Kajino, T., Mathews, G. J., & Otsuki, K. 2001, *ApJ*, 554, 578
- Wanajo, S., Itoh, N., Ishimaru, Y., Nozawa, S., & Beers, T. C. 2002, *ApJ*, 577, 853
- Wanajo, S. 2006, *ApJ*, 647, 1323
- Woosley, S. E., Wilson, J. R., Mathews, G. J., Hoffman, R. D., & Meyer, B. S. 1994, *ApJ*, 433, 229

TABLE 1
MODEL PARAMETERS AND RESULTS

| Model | R_2 (km) | $L_{\nu 2}$ (10^{51} ergs s $^{-1}$) | \dot{M} (10^{-6} M_{\odot} s $^{-1}$) | ρ_{13} (10^7 g cm $^{-3}$) | T_{13} (10^{10} K) | s ($N_A k$) | τ_{dyn} (ms) | Y_n/Y_h | $\langle A_h \rangle$ |
|------------------|---------------|---|--|--|----------------------------|--------------------|-----------------------------|-----------|-----------------------|
| A1 | 10 | 1.0 | 3.86 | 3.49 | 2.06 | 117 | 14.1 | 6.01 | 107 |
| A2 | 10 | 2.0 | 13.3 | 5.98 | 2.35 | 103 | 7.20 | 8.16 | 109 |
| A3 | 10 | 3.0 | 27.4 | 8.10 | 2.54 | 95.5 | 4.99 | 6.02 | 107 |
| A4 | 10 | 4.0 | 46.0 | 9.75 | 2.66 | 90.7 | 3.90 | 6.02 | 107 |
| A5 | 10 | 5.0 | 68.7 | 11.9 | 2.80 | 87.0 | 3.26 | 10.3 | 111 |
| B2 | 12 | 2.0 | 4.88 | 2.68 | 1.88 | 131 | 7.45 | 18.0 | 118 |
| B3 | 12 | 3.0 | 5.84 | 2.08 | 1.73 | 145 | 4.44 | 38.9 | 135 |
| B4 | 12 | 4.0 | 6.84 | 1.65 | 1.61 | 161 | 2.72 | 80.7 | 170 |
| B5 | 12 | 5.0 | 7.93 | 1.15 | 1.46 | 180 | 1.65 | 176 | 230 |
| B5a ^a | 12 | 5.0 | 5.84 | 2.07 | 1.74 | 147 | 4.37 | 39.8 | 136 |
| B5b ^b | 12 | 5.0 | 6.89 | 1.64 | 1.60 | 162 | 2.61 | 86.9 | 174 |
| C2 | 15 | 2.0 | 4.15 | 3.37 | 1.99 | 127 | 9.76 | 12.1 | 113 |
| C3 | 15 | 3.0 | 4.41 | 3.25 | 1.94 | 136 | 7.08 | 20.9 | 120 |
| C4 | 15 | 4.0 | 4.68 | 3.25 | 1.90 | 147 | 5.15 | 34.7 | 131 |
| C5 | 15 | 5.0 | 4.97 | 3.10 | 1.84 | 159 | 3.69 | 58.3 | 153 |
| D2 | 20 | 2.0 | 3.93 | 3.45 | 2.04 | 122 | 11.9 | 8.43 | 109 |
| D3 | 20 | 3.0 | 4.00 | 3.53 | 2.04 | 127 | 10.2 | 11.3 | 112 |
| D4 | 20 | 4.0 | 4.08 | 3.50 | 2.02 | 132 | 8.69 | 14.9 | 115 |
| D5 | 20 | 5.0 | 4.15 | 3.48 | 2.01 | 137 | 7.43 | 19.3 | 119 |

^aSame as B5, but without enhancement of $\dot{q}_{\nu\nu}$ for $r > R_2$.

^bSame as B5, but with enhancement of only $\dot{q}_{\nu\nu}$ for $r > R_2$.

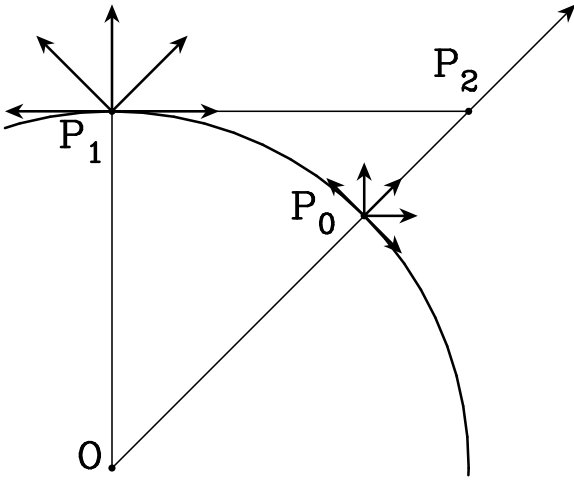


Fig. 1.— Illustration of asymmetric neutrino emission. O is the center of the neutron star. Strong neutrino emission from the “hot spot” near the point P_1 on the neutrino sphere is assumed, otherwise being isotropic. A wind blowing from a nearby point P_0 with the (weaker) isotropic neutrino emission (L_ν) suddenly see a larger number of neutrinos ($L_{\nu 2}$) when passing P_2 .

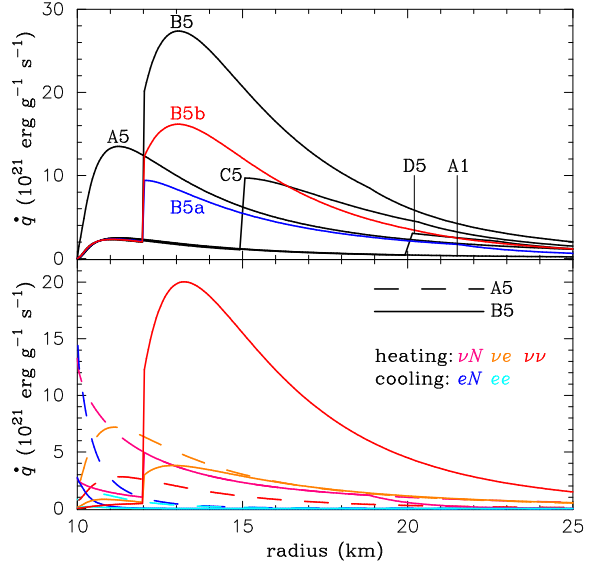


Fig. 2.— *Top*: Net neutrino heating rates for wind models A1, A5, B5, B5a, B5b, C5, and D5 listed in Table 1, as a function of r . Jump of the heating rate at $r = R_2$ is due to the sudden increase of effective neutrino luminosity from L_ν to $L_{\nu 2}$. *Bottom*: Heating ($\dot{q}_{\nu N}$, $\dot{q}_{\nu e}$, and $\dot{q}_{\nu \nu}$) and cooling (\dot{q}_{eN} and \dot{q}_{ee}) rates as functions of r . Dashed and solid lines are for wind models A5 and B5 (listed in Table 1), respectively.

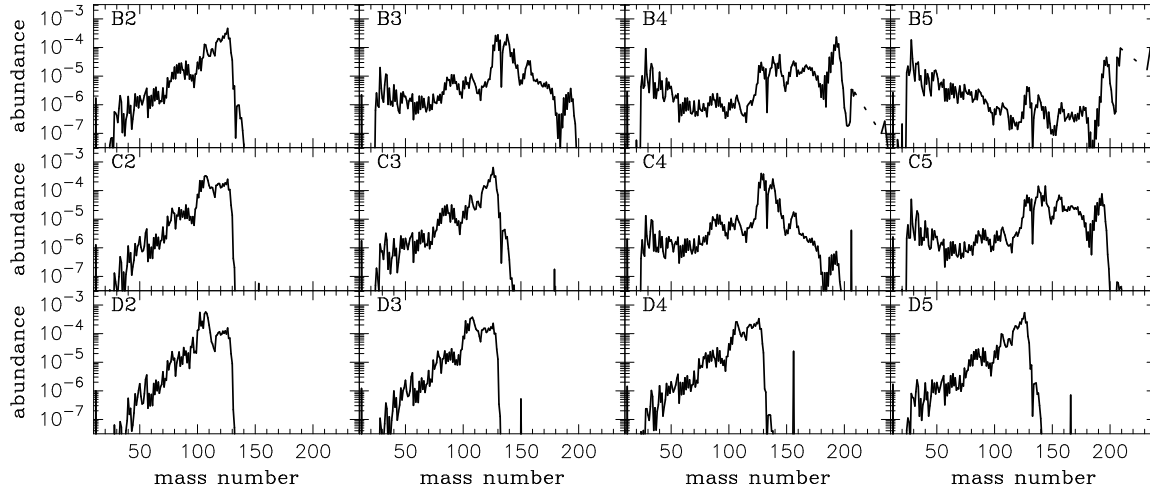


Fig. 3.— Final abundances obtained by the nucleosynthesis calculations for wind models listed in Table 1 (except for A1-A5) as a function of atomic mass number.